Thin Solid Films 715 (2020) 138429

Contents lists available at ScienceDirect

Thin Solid Films

journal homepage: www.elsevier.com/locate/tsf

The influence of glass substrates on the damp heat degradation of ZnO:Al films

Mirjam Theelen [a,*], Vasileios Ntinas [a], Henk Steijvers [a], Hero't Mannetje [a], Zeger Vroon [b]

[a] TNO Solliance, High Tech Campus 21, 5656 AE Eindhoven, The Netherlands
[b] TNO Brightlands Materials Center, Urmonderbaan 22, 6167 RD Geleen, The Netherlands

ARTICLE INFO

Keywords:
Damp heat
Degradation
Glass
Resistivity
Sodium
Aluminum doped zinc oxide

ABSTRACT

Aluminum doped zinc oxide (ZnO:Al) films were deposited by sputtering on borosilicate glass (sodium poor) and soda lime glass (sodium rich). These films were exposed up to 1032 hours of damp heat (85 °C/85 % relative humidity) to study the influence of among others the sodium content of the substrate on the ZnO:Al stability. A decrease in mobility, an increase in resistance and small changes in carrier concentration and absorption at wavelength ranges from 1500-2400 nm were observed for both types of samples. Furthermore, small spots were formed on the surface after damp heat exposure on both types of samples. Moreover, the sodium rich samples displayed whitening of all edges, due to the formation of fractal-like structures. No further differences between the sample types were observed.

1. Introduction

Zinc oxide (ZnO) has been investigated extensively because of the increasing number of possible industrial applications. Being a wide band gap semiconductor, zinc oxide is an important material for gas sensors, transparent electronics and thin film solar cells. For chalcopyrite based thin film photovoltaic (PV) devices, like $Cu(In,Ga)Se_2$ (CIGS), aluminum doped ZnO (ZnO:Al) is often used as a front contact, since it is a non-toxic, inexpensive and abundant. Furthermore, ZnO:Al is very attractive for CIGS PV, since sputtering allows room temperature deposition, which prevents exposure of the underlying layers to elevated temperatures.

However, ZnO:Al is also known to be one of the factors leading to degradation of CIGS PV devices [1]. Earlier studies have shown that this material is sensitive to the diffusion of moisture and CO_2 [2]. It was proposed that the potential barriers at the grain boundaries increased, leading to a reduction of conductivity [1,3].

It was also observed that many factors influenced the stability of ZnO:Al, leading to degradation rates under damp heat conditions that differed five orders of magnitude, from 2×10^{-8} to 4.4×10^{-3} Ωcm h^{-1} [3]. Effects that were observed to influence the degradation rate, were the film thickness [4,5,6], deposition temperature [1,5], post annealing treatments [7], crystallinity [1,5], substrate roughness [8,9] and carrier concentration/doping content [5,10].

However, in those studies, the chemical composition of the substrates was not taken into account: often relatively inert materials, like silicon wafers or borosilicate glass were selected as substrates, to prevent interaction between the substrate and the film. However, in CIGS devices, the ZnO:Al is deposited on top of a sodium containing stack: this element is in all cases present in the CIGS absorber, while in some cases even large quantities of sodium are present in the substrate [11].

In an earlier study [12], high quantities of sodium were detected in the ZnO:Al layers of CIGS solar cells degraded in the presence of an internal electric field. In these cases, a strong increase in series resistance of the solar cells was observed, indicating an increase in the film resistivity. This effect was not observed for solar cells without sodium. However, the exact effect of sodium and other elements in the substrate on film resistivity is not yet known, while it is also unknown whether sodium migrates into the ZnO:Al without an external electrical bias. In order to obtain long term stable CIGS modules as well as other opto-electronic devices, more understanding is required. Therefore, knowledge about the influence of the substrate composition on ZnO:Al stability should be obtained, based on a model system with only ZnO:Al on glass.

In this study, we present the influence of the substrate on the damp heat stability of ZnO:Al films deposited on two types of glass: soda lime and borosilicate glass, which are respectively rich and poor in sodium. The electrical, optical and compositional properties of these films have

* Corresponding author.
E-mail addresses: mirjam.theelen@tno.nl, mirjamt@gmail.com (M. Theelen).

https://doi.org/10.1016/j.tsf.2020.138429
Received 30 March 2020; Received in revised form 24 September 2020; Accepted 21 October 2020
Available online 8 November 2020

been determined before, during and after degradation. Similarities and differences on the degradation behavior of these films as well as potential degradation mechanisms are proposed.

2. Experimental procedure

2.1. Sample preparation

ZnO:Al films were deposited by radio frequency (rf) magnetron sputtering using a vertical MRC 643 sputtering tool. The films were sputtered on 10 × 10 cm^2 soda lime glass (of 1.0-mm thickness) and on Corning ''Eagle XG'' AMLCD glass (of 0.75-mm thickness) from a ZnO ceramic target with 2% Al_2O_3 by weight. After pre-sputtering, flow of pure Ar gas was set to 15 sccm. The chamber pressure was 0.4 Pa, while the rf power was 1000 W. During deposition, the samples were linearly moved back and forth during the sputtering simulating an in-line process. The films were deposited during ten scans. All deposition conditions were the same for films deposited on both substrates. The two glass substrates were each cut into 19 separate samples with various sizes for the different analysis techniques. The substrates were not intentionally heated.

Further in the text, the ZnO:Al films deposited on soda lime glass will be referred to as "Sodium rich" (SR), while the films on Corning XG will be called "Sodium poor" (SP) samples, to reflect the sodium contents in the substrates.

2.2. Degradation parameters

The samples were submitted to damp heat tests, according to certification standard IEC 61215 [13], which prescribes 1000 hours exposure to damp heat (85 °C and 85 % relative humidity (RH)). The damp heat tests were performed in a temperature and humidity controlled chamber (Espec Humidity Cabinet LHU-212M) with a humidity supply based on demi water. The samples were horizontally placed up to 1032 hours at 85°C/85% RH in varying time intervals, after which they were removed from the climate chamber and analyzed. The intervals in the climate chamber varied in magnitude to optimally follow the degradation behavior. The exposure periods were 24/24/24/24/24/24/24/24/24/72/24/72/168/216/240 hours, which sums up to the 1032 hours. The increase in the exposure period during the experiment is justified by experience that changes are stronger in the initial stage.

The samples were characterized by different analysis techniques (see section 2.3) before, during and after the damp heat test. When the samples were not in the climate chamber or measured, they were stored in an inert atmosphere (argon filled MBraun Unilab glovebox) or wrapped in a container that was evacuated to low pressure.

2.3. Characterization of film properties

The samples were characterized by a number of techniques before, during and after degradation. A PhysTech RH2010 Hall effect measurement tool, a Jandel Engineering Cylindrical four-point Probe and a Veeco Dektak 8 advanced development profiler were used to determine Hall mobility and carrier concentration, resistivity and thickness of the film respectively. Four point probe measurements were executed on 21 samples during the whole experiment on three (15 × 15 mm^2 samples used for SEM and Hall measurements) or five (20 × 30 mm^2 and larger samples) positions per sample. Measurements were repeated on the same positions. The optical properties were determined by a Shimadzu UV-3600 UV-VIS-NIR, which allowed analysis of the transmittance and reflectance of the ZnO:Al samples including the glass. From these data, absorption was calculated. The analyses were executed in the middle of the samples, not taking into account the edges. A Leica Wild M400 macroscope and a digital camera were used to determine the visual changes.

The morphological, structural and compositional properties of the films were determined by a Zeiss Crossbeam 550 focused ion beam (FIB) scanning electron microscope (SEM) coupled with an Oxford Instruments X-Max 150 Energy Dispersive X-ray Spectroscopy (EDX) tool. For the EDX measurements, the accelerating voltage was put up to 15 kV. FIB imaging was done at 30 kV and 50 pA. Milling was done using various probe currents ranging from 7 nA to 700 pA.

TOF-SIMS surface analysis was performed using a Bi^+ ion beam in both positive and negative mode. Depth profiles have been measured using a Bi^+ ion beam for analysis and 2 keV O_2^+ and 2 keV Cs^+ ion beams for sputtering in positive and negative mode, respectively. For sputtering a 250 × 250 μm^2 raster was used. The centers of the craters (50 × 50 and 100 × 100 μm) were used for collecting the data. The measured intensities are semi-quantitative, i.e. the ratios can be compared quantitatively between similar samples or measurement locations, with a typical precision of ±10%. Roughness measurements were executed by Atomic Force Microscopy (AFM) on a Park NX10 AFM on 2 × 2 μm areas.

The Hall, four point probe, microscopy, Dektak and optical properties were determined before, during and directly after exposure, while the AFM, FIB-SEM-EDX, ToF-SIMS and confocal measurements were executed after long term storage in a glovebox.

3. Results

3.1. Initial parameters

Table 1 displays the initial parameters of the sodium rich and sodium poor films. Small differences in the thickness and electrical parameters of the films were observed. The SR generally slightly outperformed the SP films for the electrical properties, while the transmission of these samples is slightly lower. A possible explanation for these small differences is the heating of the samples: even though deposition was executed at room temperature, the sputtering plasma might have heated the samples, which might have be different for the two types of substrates, e.g. due to the small difference in thickness. The differences in substrates might also have impacted the microstructure and the number of grain boundaries in the samples. However, no strong differences were observed in cross-section SEM measurements (not depicted).

3.2. Visual and compositional observations

Before exposure to damp heat, all samples appeared homogeneous (Fig. 1) and had a transmission of 78-80% (including the absorption of the glass). Due to damp heat exposure, small white spots have occurred on both the sodium poor and the sodium rich samples. This is analogue to spots earlier observed in reference [1].

The largest difference between the two sample types was found on the edge of the samples (Fig. 1). While the sodium poor samples showed the occurrence of a very thin white line at the edges, all SR samples have a white edge with a thickness of one to several millimeters. The thickness was independent of the size of the samples, so both the small and the larger samples had comparable edges. The microscopy images showed that the white edge contained 'fractal'-like lines.

AFM studies were used to check the surface roughness on the 'clean' areas. Therefore 2 × 2 μm^2 areas were measured on both types of glass substrates and degraded and non-degraded ZnO:Al films. On all measured surfaces, the root mean square (rms) values were between 0.3 to 2.6 nm, indicating all samples were relatively smooth. Naturally, when larger areas were taken into account, the rms values increased due to the inclusion of the surface spots and edges.

3.3. Electrical changes

Fig. 2 shows the development of the sheet resistance of 21 samples. The red and blue figures represent the sodium rich and sodium poor samples respectively. On a first glance, the increase in sheet resistance seemed slightly higher for the sodium poor samples.

Table 1
Initial parameters of the sodium rich (SR) and sodium poor (SP) films.

Parameter	Technique	SR	# measurement points	SP	# measurement points
Thickness	Dektak	496±16 nm	4	451±13 nm	4
Sheet resistance	4 PP	11.0±0.8 Ω/□	81	15.1±1.0 Ω/□	80
Sheet resistance	Hall	10.0±0.2 Ω/□	3	14.0±0.2 Ω/□	3
Carrier concentration	Hall	(5.23±0.03) 10^{20} cm^{-3}	3	(4.69±0.04) 10^{20} cm^{-3}	3
Mobility	Hall	23.9±0.5 cm^2/Vs	3	21.0±0.3 cm^2/Vs	3
Resistivity		5*10^{-4} Ω cm		6-7*10^{-4} Ω cm	
Transmission (350-1200 nm)	NIR-UVVIS	78.2±0.5%	3	79.9±0.1%	3
Absorption (350-1200 nm)	NIR-UVVIS	12.9±0.5%	3	10.7±0.1%	3

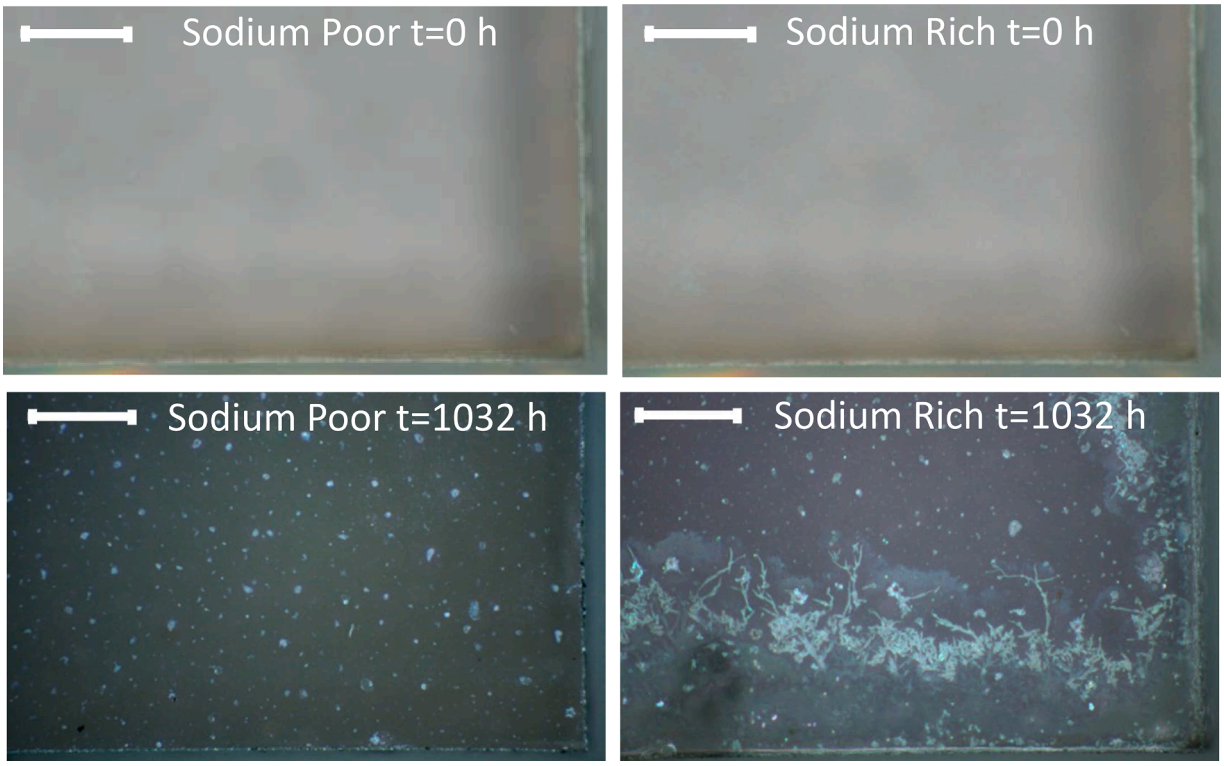

Fig. 1. Optical microscope images of the bottom right corner of ZnO:Al deposited on sodium poor and sodium rich substrates before and after the damp heat exposure. The size bar represents a length of 1 mm.

In order to quantify the increase in sheet resistance, the values were fitted with a square root function, following:

$$y = a * \sqrt{(bt)} + y_0 \quad (1)$$

These fits are shown as the red and blue lines in Fig. 2. The results are displayed in Table 2. The table and the figure show that the increase in series resistance could be well fitted by a square root function. These fits also display that no clear differences between the conductivity decrease of the SR and SP samples could be observed.

Hall-van der Pauw measurements were performed in order to study the development of the mobility and carrier concentration on two SR and two SP samples (Fig. 3). The development of the sheet resistance is, as expected, similar to the values obtain from four point probe measurements. The change in resistivity is not depicted, but naturally has the same shape. The increase in resistance is mostly driven by a decrease in Hall mobility, which curve seems to have a similar shape. A smaller decrease was observed for the carrier concentration. These effects are similar to the performance changes as presented in reference [1].

3.4. Optical changes

All samples were measured by optical spectroscopy in the middle area before and after damp heat exposure (Fig. 4). Since the edges were not included, the impact of the spots was taken into account, while the edge changes were not.

Fig. 4 shows that barely any changes occurred in the ultraviolet (UV), visible and near infrared (IR) range: for photons with a wavelength above 1500 nm, a decrease in reflection and an increase in absorption was observed, similar to references [1,8,14]. In reference [14], this effect was observed for a part of the measured samples (flat substrates with ZnO:Al films of 433 and 869 nm). The transmission of these samples is constant, also in the wavelength region above 1500 nm.

These results indicate that the optical changes of SP and SR samples due to damp heat exposure are limited and similar for both types. An exception will likely exist for the edge of the samples. The sodium and other differences in substrate composition and morphology did thus not impact the optical properties in the middle of the samples.

3.5. Compositional and morphology changes

In order to define the compositional properties of the "bulk" of the ZnO:Al films (the regions where no large spots and fractals were observed), ToF-SIMS measurements were executed. Fig. 5 displays the spectra of both SP and SR samples before and after exposure to damp

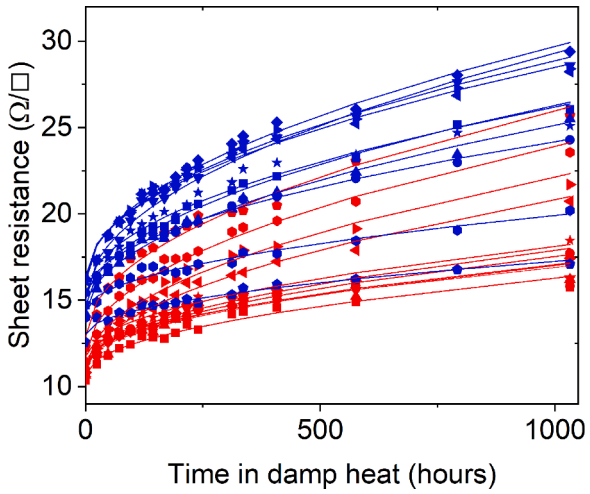

Fig. 2. Development of sheet resistance of 21 samples. All samples are measured on three or five positions. Standard deviations are omitted for clarity. The red and blue points represent respectively the sodium rich and sodium poor samples. The lines are fits based on a square root function, following equation (1).

Table 2
Average values and standard deviations for the 21 fits of the development of the sheet resistance. The median R^2 of these fits is 0.98.

	a	b	y_0
Sodium poor	0.61±0.08	0.29±0.11	15.1±1.0
Sodium rich	0.56±0.07	0.21±0.10	11.4±0.6

heat conditions taken in positive mode. It should be noted that the intensity differences between different elements and between the same element in different matrices cannot be compared. This is for example visible in the aluminum signal, which is higher than the zinc signal, while the zinc content is significantly higher in these samples. On the other hand, differences in quantities of one element in a similar matrix provide an insight of concentration differences.

The ToF-SIMS spectra before exposure show a high sodium and potassium content in the glass of the SR samples (Fig. 5c). These elements are present in strongly reduced quantities in the SP samples (Fig. 5a). Sodium is present in the bulk of the ZnO:Al films in both the SP and SR samples, likely in low quantities. After exposure to damp heat, the sodium content in the SR ZnO:Al films has increased slightly (Fig. 5d), especially near the front of the sample. No significant change could be observed for the SP samples (Fig. 5b). The silicon content has also increased in the SR samples at the front, while a minor increase was observed in the SP samples.

Measurements taken into the negative mode (not depicted) displayed the presence of OH^-, Cl^-, H^-, SiO_2^-, CN^- and C_2^- fragments in a degraded SR sample. This especially occurred close to the front, while the ZnO^- intensity decreased in this region. Similar results are reported and displayed in reference [1]. This indicates that 'foreign' species, like H_2O, chlorine and CO_2 have migrated into the ZnO:Al film. Part of these species, like silicon, might also have resulted from tiny spots still present in these "clean" areas.

Apart from changes in the bulk of the ZnO:Al films, the spots and fractals were also studied in depth. Confocal measurements were used to study the topological properties of these features. Fig. 6(a) displays the confocal measurements in the middle region of a degraded SP sample. This shows that the spots are actually islands on top of the film. These islands can be several hundreds of nanometers up to even a micrometer in height and occur for both the SR and the SP samples. Fig. 6(b) shows that the edges of the SR samples are also elevated above the ZnO:Al

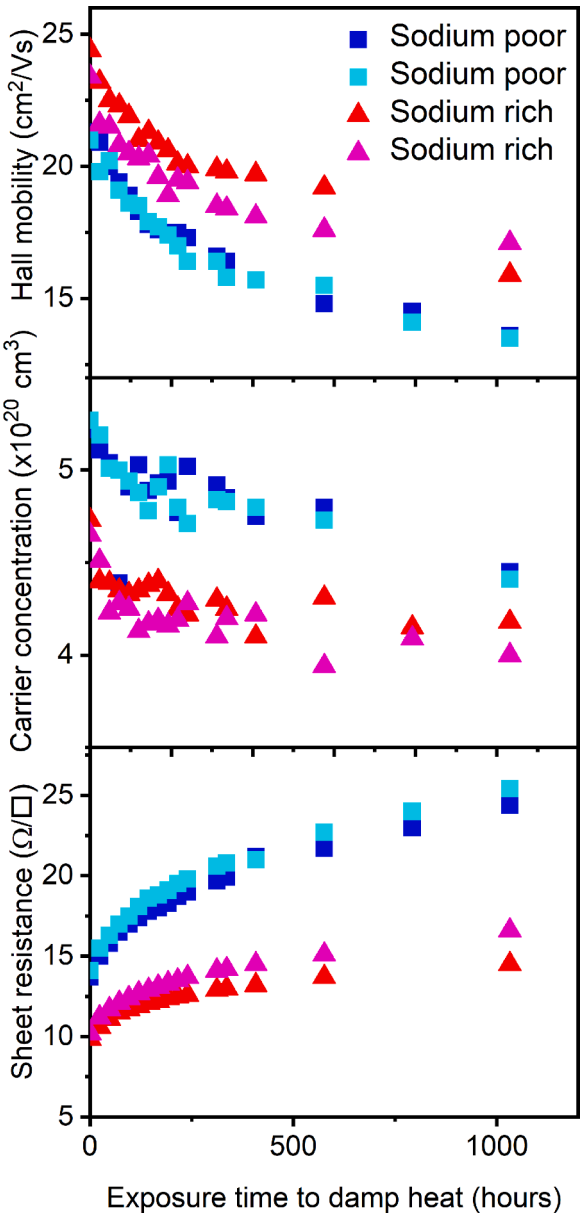

Fig. 3. Hall mobility, carrier concentration and sheet resistance as obtained by Hall measurements as a function of exposure time to damp heat treatment time for ZnO:Al deposited on sodium poor (blue) and sodium rich (red/pink) substrates.

surface. It is likely that the white areas correspond with the peaks, which could be several micrometers in height. In some case, it seems like the ZnO:Al film around the fractal was lower than the surrounding ZnO:Al film.

The spots as well as the edges were further studied by SEM-EDX for compositional and morphological information. Fig. 7 shows a SEM image of the surface of the SR sample. These measurements displayed that the spots were not homogeneous, but varied in appearance. Most spots are relatively large circles, while the larger spots contained darker 'nuclei'. EDX measurements demonstrated that the spots contained increased levels of carbon, chlorine, silicon and calcium, but very large differences in composition were found. Since it is hard to detect sodium in a zinc based matrix, the presence of this element could neither be proven nor rejected.

The nuclei were studied in more detail by FIB SEM-EDX. A cross-section of one of the nuclei is displayed in Fig. 8. EDX revealed that this specific nucleus contained both carbon and silicon. The presence of

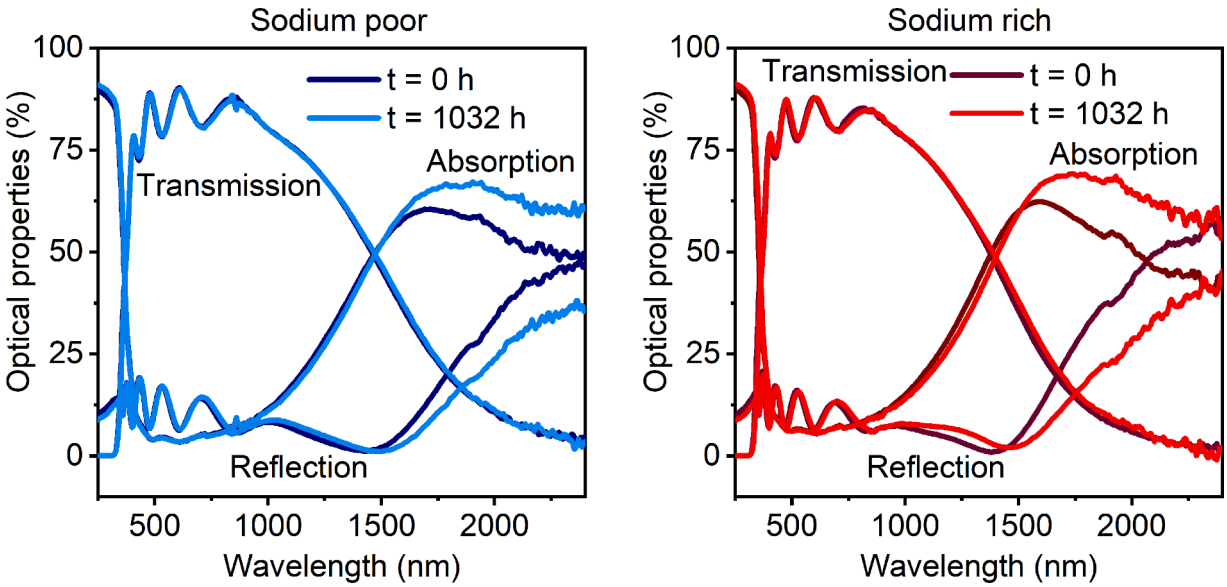

Fig. 4. Optical properties of ZnO:Al on a (left) sodium poor and (right) sodium rich substrate before and after damp heat exposure

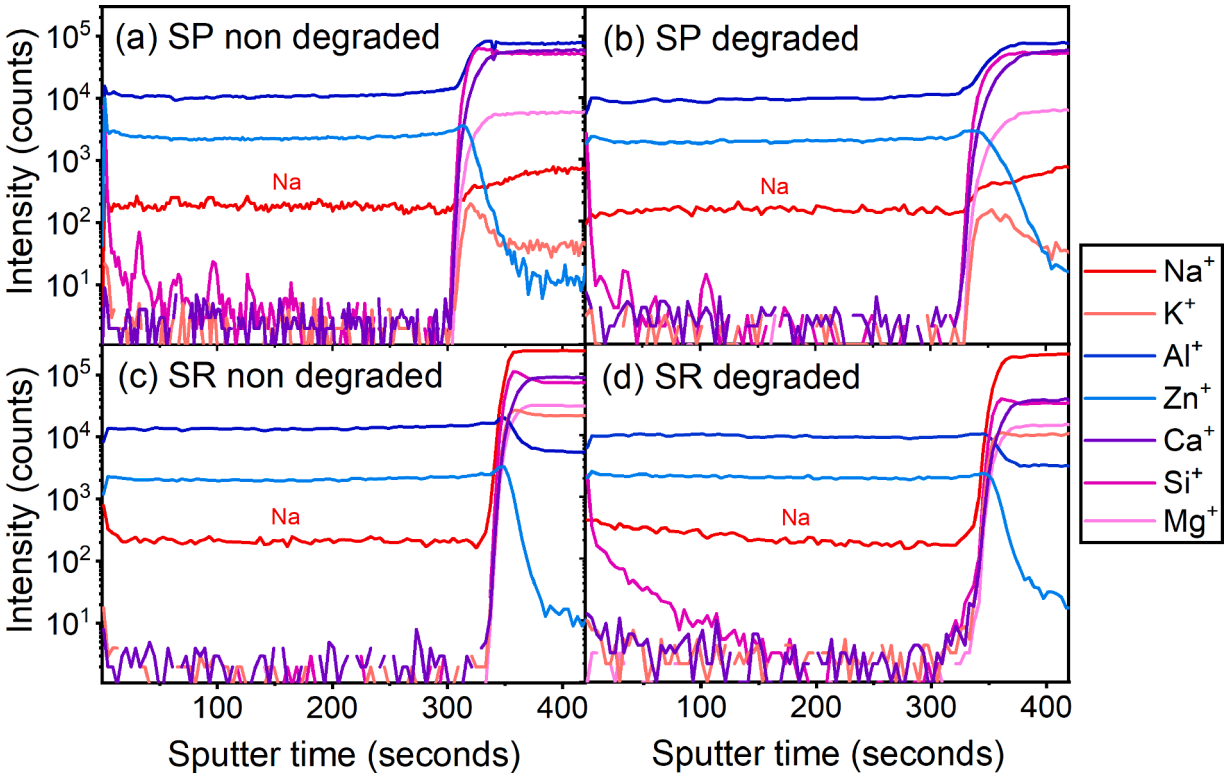

Fig. 5. ToF-SIMS measurements in positive mode of the ZnO:Al films on glass in areas with no clear surface modifications like spots or fractals (a) Sodium Poor non-degraded (b) Sodium Poor degraded (c) Sodium Rich non-degraded and (d) Sodium Rich degraded.

the nucleus actually seemed to have modified the morphology of the ZnO:Al film: voids have occurred in the ZnO:Al layer at the interface with the nuclei. This indicates local dissolution of the ZnO:Al layer, likely starting from the grain boundaries. It was observed that only the top part of the ZnO:Al was affected, while the bottom part still looked intact. It should be noted that the total area covered by the nuclei is small.

Fig. 9 shows the composition of the white edge of the degraded SR samples. In the bulk of the material, zinc (possibly sodium), oxygen, aluminum and silicon were observed. These bulk materials are 'blocked' on the positions of the elevated 'fractals' laying on top of the ZnO:Al films. These 'fractals' were demonstrated to be rich in carbon and possibly sodium. It should be noted that separation of the zinc and sodium signals is complicated, so the presence of the latter is not ambiguously proven. From these measurements, it is hard to conclude whether the fractals also contain oxygen, since this is a very major component of both glass and ZnO:Al. Compared to the variation in nature of the spots, the fractals have a relatively constant composition, with strongly elevated carbon levels (50-80 atomic %) compared to 22% on the reference level.

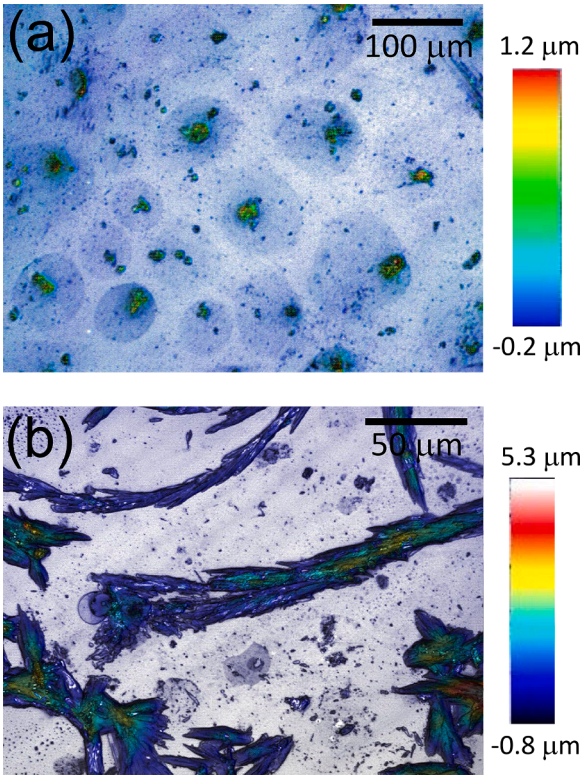

Fig. 6. Confocal microscopy images of samples exposed to damp heat for 1032 hours and glovebox storage on (a) the spots in the middle of a sodium poor sample and (b) the edge of a sodium rich sample. All values are given in µm, note the difference in color scales.

Spots are also visible in the SEM image in Fig. 9, while on this scale the spots are barely visible on the EDX maps. An exception exists for the spots in the bottom right corner, which show a small increase in oxygen and silicon levels.

The spots and fractals were also studied by ToF-SIMS. An example of measurements on spot positions is shown in the concentration maps of Na^+ in Fig. 10. These images display the concentration of Na^+ through the depth of three sample positions: a spots on a degraded SR sample, a fractal on this same sample and a spot on a degraded SP sample. While the fractals have a very high Na^+ content, the spots on the SR sample also contain relatively large amounts of Na^+. Small quantities of Na^+ were also observed on the spot on the SP samples.

Apart from the Na^+ content, Fig. 11 shows positive mode cross-section ToF-SIMS measurements on three areas on a degraded SR ZnO:Al film. The locations are indicated in Fig. 10, where [b], [s] and [f] represent respectively the background, spot and fractal areas. Due to the small collection areas, the absolute counts are significantly lower than in the graphs in Fig. 5 (e.g. ~3k vs ~240k Na^+ counts for the glass in the SR samples), while the shape of the curve is similar.

Fig. 11(b) shows that on the spot, enhanced levels of Na^+, K^+, Mg^+, Ca^+ and Si^+ were found. The Zn^+ and Al^+ signals are lower at this position, especially at the front of the sample, indicating that the additional ions are mostly located on top of the ZnO:Al film.

Finally, the measurements on a fractal are displayed in Fig. 11(c). In this graph, the glass/ZnO:Al interface was not reached, so only data for the fractal and potentially the ZnO:Al film is displayed. It contains very high quantities of Na^+, leading to a saturated signal. K^+ is also present in high quantities, again majorly towards to front of the film.

A measurement on a spot in the negative mode (Fig. 12) displayed very high quantities of fragments from 'environmental' species, like Cl^-, OH^-, H^-, CN^-, CHO_2^- and C_2^- as well as SiO_2^-. These fragment were especially present in high concentrations near the front. Compared to the degraded non-spot areas, these fragments had up to 50 times higher counts. The ZnO^- and AlO^- fragments showed a decrease in occurrence

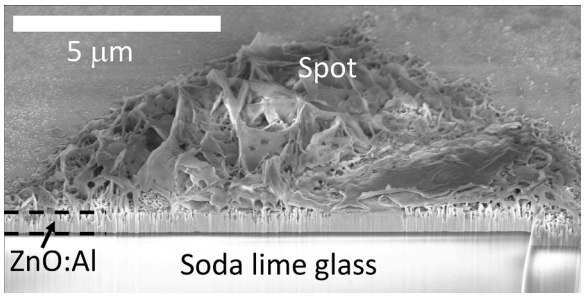

Fig. 8. Cross-section SEM image of ZnO:Al deposited on a sodium rich substrate after 1032 hours exposure to damp heat and glovebox storage. The cross-section was obtained by FIB preparation.

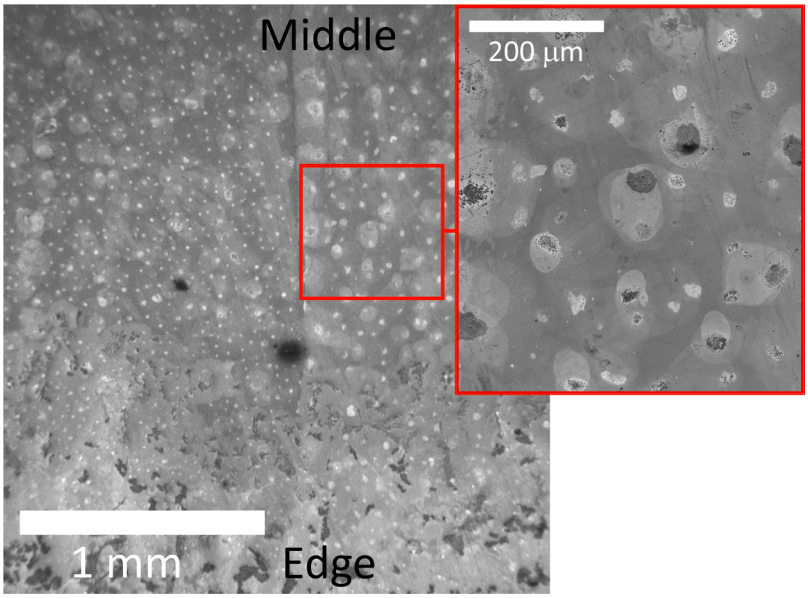

Fig. 7. SEM image of SR ZnO:Al film after 1032 hours exposure to damp heat and glovebox storage.

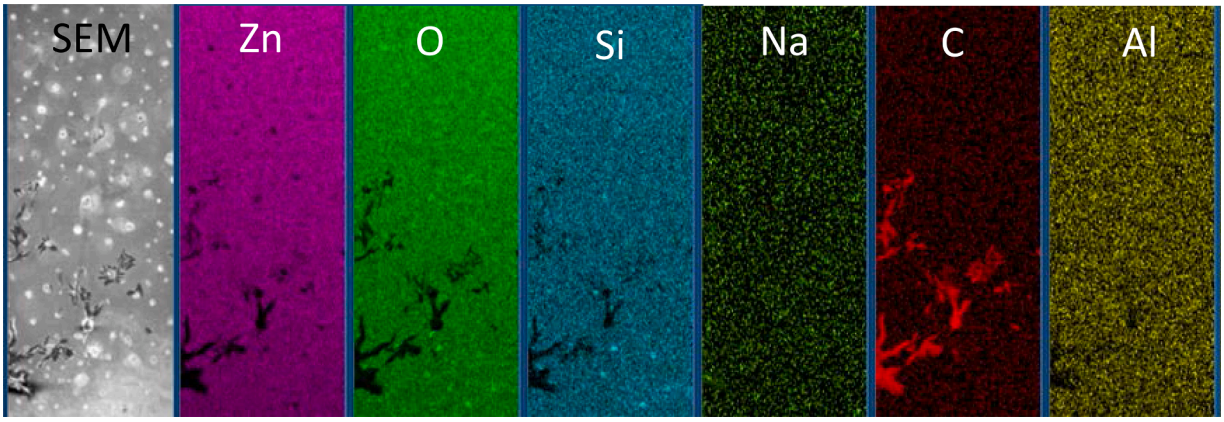

Fig. 9. SEM-EDX measurements on the edge of an ZnO:Al deposited on sodium rich substrate after 1032 hours exposure to damp heat and glovebox storage. The width of these images is 387 μm.

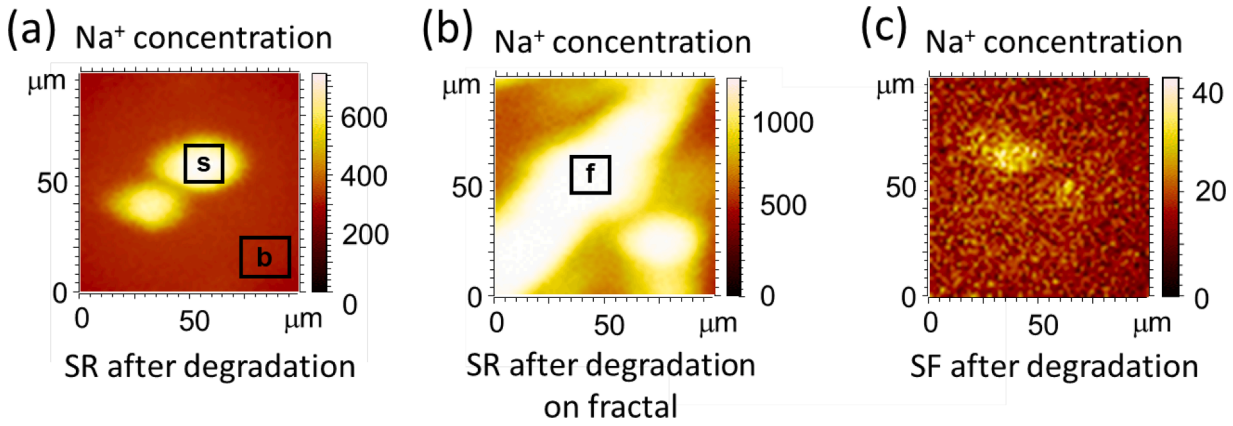

Fig. 10. Concentration maps of Na^+ as obtained by ToF-SIMS (a) SR sample with spot, after degradation (b) SR sample with fractal after degradation (c) SF sample with spot after degradation. It should be noted that the color scale is different for the individual concentration maps. The boxes in the figure represent the measurement areas of the background [b], spot [s] and fractal [f] graphs in Fig. 11. For figures (a) and (c) the complete film was measured, while the glass was not reached for figure (b).

near the front. It should be noted that the CN^- and CHO_2^- fragments displayed mass interference with respectively ^{10}BO and $^{11}BH_2O_2$, resulting in some intensity in the glass substrates.

4. Discussion and conclusion

The ZnO:Al films on sodium poor and sodium rich glass degraded due to damp heat exposure. This lead to the appearance of two types of features:

- Occurrence of **surface spots**: these spots are islands on top of the ZnO:Al surface, with various appearances (Fig. 13 bottom left). The formation of spots occurred for both sodium rich and sodium poor samples. Their composition varied per spot, but they can be rich in silicon, calcium, potassium, sodium, hydroxide, organic species and chlorine, which are likely deposited in very small quantities from the air and demineralized water. Although the used water was purified, very small quantities of pollution are always present, while small particles 'dust' are always present in the air. A possible explanation is the placement of cold samples in a pre-heated 85°C/85% RH chamber, leading to condensation of liquid water. After heating of the sample, the water might have evaporated, leaving behind ions, molecules and particles. It is thus likely that this effect will be very limited in packaged devices. Apart from species from the environment, it is likely that sodium has partly originated from the substrate: Fig. 10 displays that SR samples contain higher concentrations of sodium on the spots after degradation than SP samples.

Within the spots, various regions could be observed, including a nucleus of micrometers in size. It was observed that the ZnO:Al film under such islands had partly disappeared, likely following the patterns of the grain boundaries. In earlier work [2], similar effects were observed for samples immersed in CO_2 rich water. Hüpkes et al. [15] have reported on severe local dissolution around the grain boundaries in the presence of water and high concentrations of CO_2. Since ZnO:Al dissolves at pH values above 12 and under 6, it is possible that the presence of (slightly) acidic species in a (liquid) humid environment led to local acidic conditions at the ZnO:Al/glass interface. Possible sources of the low pH can be CO_2 from the air as well as very low concentration of contamination in the demineralized water. It is likely that this effect occurred directly during the damp heat exposure, but it could also have happened during long-term inert storage. In that case, water as well as other species might have been 'stored' locally in the spots.

Generally, the effect of the spots on the optical properties (at least up to 1500 nm) is negligible. Since the spots are on top of the film,

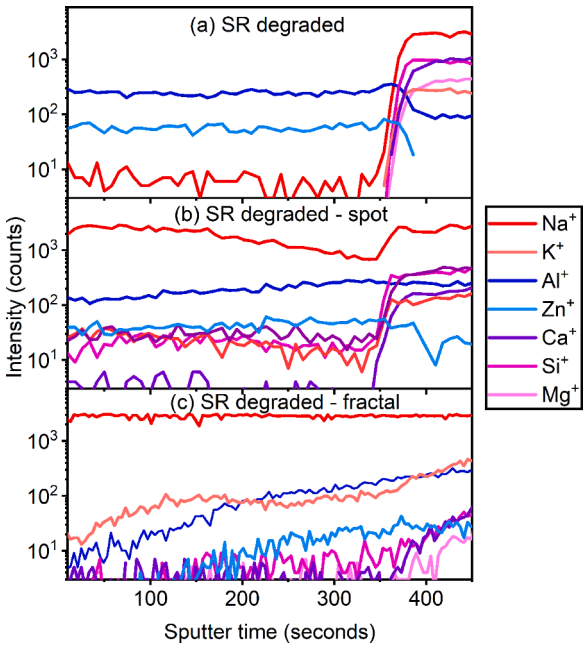

Fig. 11. ToF-SIMS measurements in positive mode of a degraded SR ZnO:Al film in an area with (a) no clear surface structures (b) a spot (c) a fractal. The locations are indicated in Fig. 10 as [b], [s] and [f] respectively.

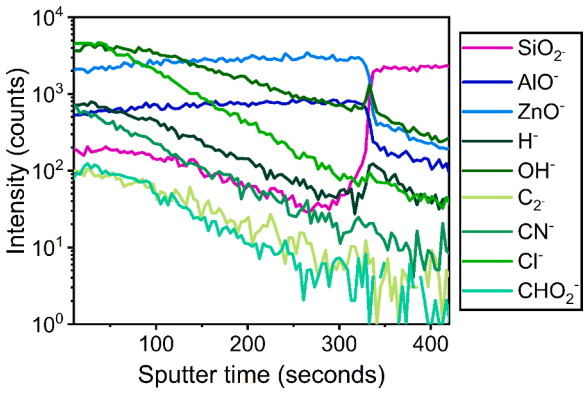

Fig. 12. ToF-SIMS measurements in negative mode of a degraded SR ZnO:Al film taken on a spot.

they will likely not strongly interfere with the electrical properties either, apart from the dissolution of material.

- Whitening of **sample edges** of the sodium rich samples, caused by the formation of fractal-like structure on top of the ZnO:Al film. These structures can be as thick as two micrometer and are rich in sodium, potassium and carbon, while oxygen can possibly also be present. Since this only happened on the SR samples and the roughness of both samples is low, it is likely related to the composition from the glass. Logical candidates for the formed material are Na_2CO_3 or analogue species like $NaHCO_3$, K_2CO_3 or $KHCO_3$, although the oxygen level of the fractal-like structure is unclear. Therefore, it is also possible that these are (alkali)carbohydrates.

  It should be noted that, apart from the different alkali content in the substrates, additional explanations exist for the presence of the white edges. One prominent example is a possible difference in microstructure between the glass substrates, causing stress differences between the films, which might have promoted ion migration.

The following effects were observed on the electrical and optical properties of the middle of the samples:

- An increase in resistivity, which can be fitted with a square root function. Due to this relationship, resistivity change can be linked with a diffusion-like process, in which a species from an infinite reservoir diffuses into a semi-porous material [1,16]. The diffusion of the species in the sample will thus be the rate-determining step, while the reaction between the diffusion species and the grain boundary atoms inside the sample is faster. The resistivity increase seemed slightly higher for the SP samples, although this could not be clearly determined for this number of samples. A higher degradation rate for the SP samples can be explained by the differences in ZnO:Al film thickness: if the diffusion rate of species would be similar in both samples, thinner (sodium poor) samples would more rapidly suffer from conductivity loss, since a larger percentage of the depth of the samples is degraded.

  This resistivity change is majorly driven by a decrease in carrier mobility, while the carrier concentration also decreased slightly. The strong decrease in the carrier mobility indicated that an increase in barrier height and/or width at the grain boundaries is likely the main cause (Fig. 13 top). This will lead to reduced electron transport, due to reduced tunneling and reduced thermionic emission [3,10]. Next to that, (ionized) impurity scattering within the grains might also have been enhanced, since the carrier concentration also displayed a small decrease.

  In the degraded film, enhanced levels of OH^-, Cl^-, H^-, SiO_2^-, CN^- and C_2^- fragments were observed. While part of these fragments might result from very small spots, it is expected that a large share has diffused in the film. Earlier work has demonstrated that this resistivity increase can be caused by the combined ingression of water as well as CO_2 [1,2,17]. Therefore, a combined ingression of H_2O and CO_2 in the grain boundaries might be the major cause (Fig. 13), while chlorine might have also played a role [2]. This effect occurred for both sodium rich and sodium poor samples. Moreover, for the SR sample, a minor increase in Na^+ to the front of the film was observed. Its impact on resistivity is unclear. Additionally, part of the ZnO:Al material was dissolved under the nuclei of spots, likely starting from the grain boundaries. This will locally have a large impact on the resistivity increase, but since the area covered by the nuclei is limited, the overall impact might be relatively small.

  The reported increase in resistivity will have the largest impact on CIGS solar cells or other optoelectronic devices, but is thus similar for both types of substrates. Generally, no indication for more rapid loss of conductivity for the middle of the sodium rich samples was observed.

- A minor decrease in the infrared (IR) reflection of the films, compensated by an increase in absorption, was observed. A similar effect was reported by references [1,8,14]. In reference [14], the optical properties of ZnO:Al films (433 and 869 nm) on smooth quartz glass were fitted with an optical model. The change in optical properties was proposed to be linked to the decrease of the Drude mobility or carrier concentration. It should be noted that the in-grain electrical properties, as obtained from optical models, can be different from the electrical properties of multiple grains, as obtained from electrical measurements. These changes might thus indicate minor changes in the in-grain mobility or carrier concentration. Another explanation can be found in the (rough) surface spots, which might absorb the light, instead of reflecting it.

  For most opto-electronic devices, this change in optical properties will not impact their performance, since the transmission of the ZnO:

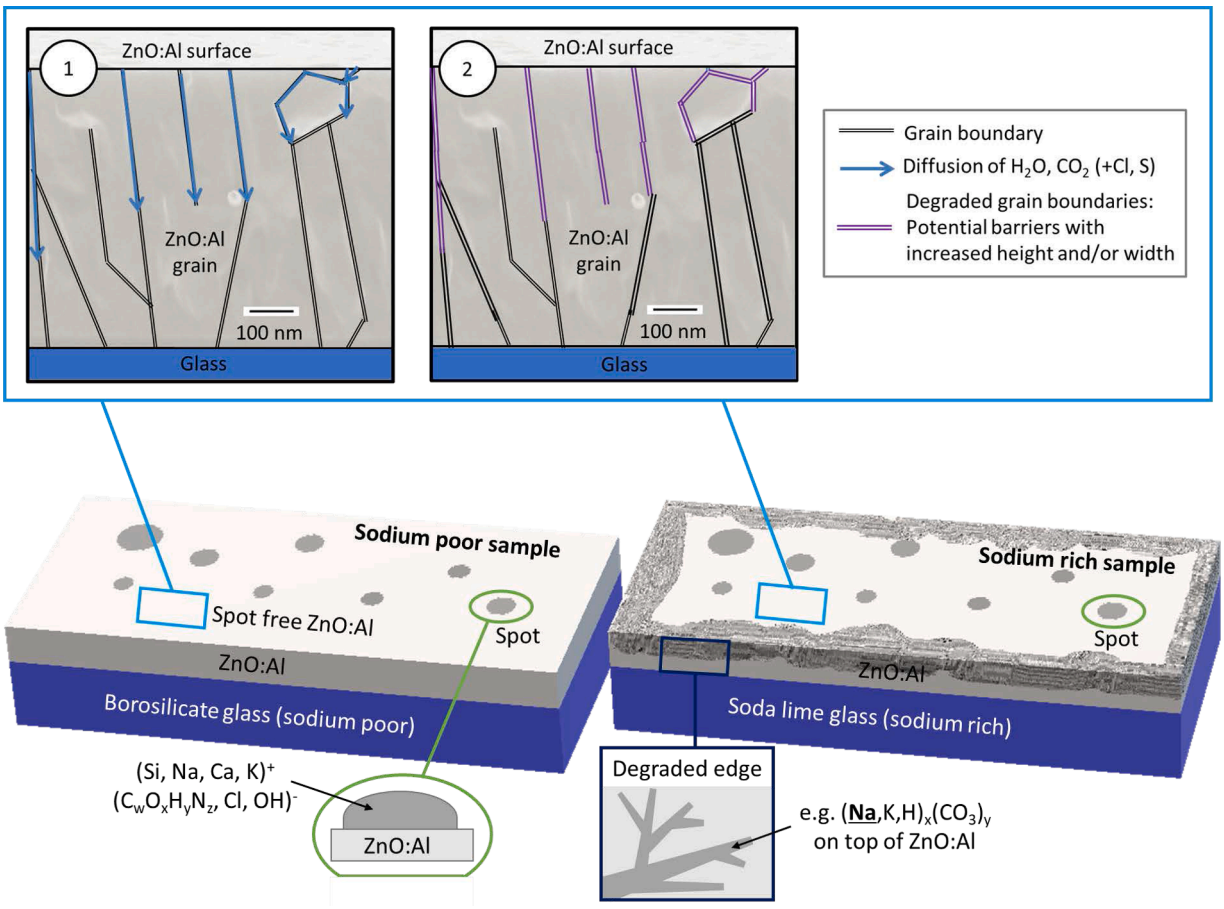

Fig. 13. Schematic representation of degradation phenomena of damp heat exposed ZnO:Al on borosilicate glass (SP) and soda lime glass (SR).

Al is still constant. Moreover, CIGS solar cells, and many other devices, only absorb light with a lower wavelengths (e.g. of 1100 nm and shorter [18]).

It is naturally important to realize that the sodium content is not the only variation between soda lime glass and borosilicate glass. However, the absence of clear difference in degradation behavior in the middle of the samples indicates that none of these variations have a strong influence.

4.1. Impact for photovoltaic devices

The increase in resistivity as observed due to damp heat exposure will naturally impact the series resistance of PV devices [3,12]. In reality, the packaging of PV devices will protect the ZnO:Al against this effect. However, in order to reach very low cost PV devices, low cost packaging materials are attractive. Therefore, cells that are intrinsically stable under the ingression of (some) humidity can allow the use of packaging material with a relatively high Water Vapour Transmission Rate. In that case it should be noted that the formation of spots is likely related to contact with (liquid) water, which would only happen in the unlikely case of complete rupturing of the packaging material.

The main differences between the sodium poor and sodium rich glass samples was found in the edge of the samples: this small degraded area was not included in the optical or electrical measurements, which were executed on large areas in the middle of the samples, so this effect was not reflected in the results. Since large scale devices will have a higher area/edge ratio, the effect of edge whitening might be smaller in real devices. Furthermore, no significant differences between the two types of substrates was observed.

It can be concluded that, without an external electrical field, no strong additional degradation effects occurred in the sodium rich samples. However, single ZnO:Al films on flat glass substrates are naturally not the same as ZnO:Al layers in functioning PV devices. When ZnO:Al films in CIGS devices are considered, the substrate roughness is higher. The underlying absorber/buffer layers can have roughness values of hundreds of nanometers or higher [19]. Greiner et al. [9] already showed that roughness of a quartz substrate can affect damp heat stability. This effect might be even larger in the presence of sodium: in case of more contact area between the sodium source and the ZnO:Al films, reported effects might be stronger. Moreover, this might also create areas that are more similar to the fractal-rich edges of the samples in this experiment.

Additionally, degradation will not only occur on or inside single films, but also at interfaces. Interaction between the layers in a device is also crucial in degradation mechanisms. Finally, the functioning of a device will also impact (ion) migration. It should therefore be noted that sodium (and potassium) migration might still occur in the presence of an electric field. Various literature sources have reported the migration of sodium to ZnO:Al films in operating CIGS devices. These effects can be found in devices degraded under two conditions:

I Simultaneous exposure of unpackaged CIGS cells to damp heat and illumination. Due to the light, the solar cells were under open circuit conditions and thus experience a (small) internal voltage. These conditions caused the migration of alkali-element, including sodium, to the pn-junction and the ZnO:Al front contact. The sodium source is

likely the CIGS absorber, while it could also have partly originated from the glass substrate [20,21].

II Potential Induced Degradation ("PID"), which is a large external voltage (e.g. -1000 V) between the cell and its packaging material (the glass and the frame). For glass-glass based CIGS devices, sodium can then migrate from both the substrate and the front glass. Since the latter is separated by an encapsulant, transport from the substrate glass will likely be faster. Various sources have demonstrated that variation in substrate glass [22] and molybdenum back contact [23] impacts the long term performance.

Under both conditions, the sodium content available from the back side of the cell was found to be important for the long term stability. Under the smaller internal biases plus damp heat (condition I), modification of the microstructure of the molybdenum back contact [21] and application of a diffusion barrier on top of soda lime glass [12] were found to be impacting the sodium migration through the cell. This happened during the high temperature absorber deposition and influenced the 'reservoir' of sodium present in the CIGS absorber available to play a role in degradation. Faster degradation occurred in the presence of a higher sodium (and potassium) content. For the PID-like high(er) voltage experiments (condition II), Fjällström et al. [22] and Salomon et al. [23] respectively showed the impact of molybdenum microstructure and glass composition on the sodium migration. In all cases, this greatly influenced the long term stability under these biases.

Both the internal bias [21] as well as the PID [23] treatments resulted in the appearance of spots on the TCO surface, in some cases with a (ruptured) nucleus, giving the spots a volcano-like appearance. These spots were also found to have elevated levels of sodium and carbon [21,23], which might also have been sodium carbonate [23]. It should be noted that these spots did not occur at samples under condition I with a sodium barrier. Although the spots reported in literature [12,21,23] have a similar size and appearance as the spots in this study, they are likely different phenomena:

In this study, the spots also occurred on ZnO:Al samples on sodium poor borosilicate glass substrates.

In this study, the spots were rich in other elements, like silicon and calcium.

However, it is interesting to note that the fractals, making up the white edges of the degraded SR samples, have a similar composition as the spots from the CIGS devices exposed to the biases. One explanation could be the relatively rough nature of the edges, which might have allowed migration of among others sodium, via the outside of the ZnO:Al films.

5. Conclusions

Sputtered thin ZnO:Al films on borosilicate glass and soda lime glass were exposed to damp heat (85°C/85% RH) to accelerate the physical and chemical degradation behavior. Optical measurements showed that the transmission of the films did not change. It was observed that the carrier concentration were slightly reduced, while the Hall mobility and thus the overall resistivity decreased. No large impact of the substrates on the conductivity loss was observed. On both types, spots were observed distributed evenly over the film. Moreover the edges of the ZnO:Al films on the SR samples has whitened, which was caused by the formation of micrometer thick fractal structures. Both defect types occurred to be rich in carbon, while the fractals were also very rich in sodium. All these effects are likely related to, among others, the ingression of water. It is therefore likely that a water barrier can at least partly prevent the described mechanisms.

CRediT authorship contribution statement

Mirjam Theelen: Conceptualization, Methodology, Validation, Formal analysis, Investigation, Data curation, Writing - original draft, Visualization, Project administration, Supervision, Funding acquisition. **Vasileios Ntinas:** Investigation, Writing - review & editing. **Henk Steijvers:** Resources, Investigation. **Hero't Mannetje:** Investigation. **Zeger Vroon:** Conceptualization, Supervision, Funding acquisition, Writing - review & editing.

Declaration of Competing Interest

The authors declare that they have no known competing financial interests or personal relationships that could have appeared to influence the work reported in this paper.

Acknowledgments

The authors would like to thank Thomas Glen, Norbert Radacsi (University of Edinburg), Hans Snijders, Bertil Okkerse (Eurofins EAG) and Karine van der Werf (TNO) for their help by the measurements or analysis. This work is supported by 'Netherlands Enterprise Agency' (RvO) and the Dutch Topteam Energy via the project 'Performance and Electroluminescence Analysis on Reliability and Lifetime of Thin-Film Photovoltaics' with grant number TEUE116203. Furthermore, the Early Research Program 'Sustainability & Reliability for solar and other (opto-)electronic thin-film devices' (STAR) from TNO is also acknowledged for funding.

References

[1] M. Theelen, T. Boumans, F. Stegeman, F. Colberts, A. Illiberi, J. van Berkum, N. Barreau, Z. Vroon, M. Zeman, Physical and chemical degradation behavior of sputtered aluminum doped zinc oxide layers, for Cu(In,Ga)Se_2 solar cells, Thin Solid Films 550 (2014) 530–540, https://doi.org/10.1016/j.tsf.2013.10.149.

[2] M. Theelen, S. Dasgupta, Z. Vroon, B. Kniknie, N. Barreau, J. van Berkum, M. Zeman, Influence of atmospheric species water, oxygen, nitrogen and carbon dioxide on the degradation of aluminum doped zinc oxide layers, Thin Solid Films 565 (2014) 149–154, https://doi.org/10.1016/j.tsf.2014.07.005.

[3] M. Theelen, F. Daume, Stability of Cu(In,Ga)Se_2 Solar Cells: A literature review, Solar Energy 133 (2016) 586–627, https://doi.org/10.1016/j.solener.2016.04.010.

[4] F. Pern, B. To, C. DeHart, X. Li, S. Glick, R. Noufi, Degradation of ZnO Window Layer for CIGS by Damp-Heat Exposure, Proc. SPIE 7412 (2008) 74120.

[5] T. Minami, T. Miyata, Y. Ohtani, T. Kuboi, Effect of thickness on the stability of transparent conducting impurity-doped ZnO thin films in a high humidity environment, Phys. Stat. Sol. (RRL) 1 (1) (2007) R31–R33, https://doi.org/10.1002/pssr.200600009.

[6] T. Minami, T. Kuboi, T. Miyata, Y. Ohtani, Stability in a high humidity environment of TCO thin films deposited at low temperatures, Phys. Stat. Sol 205 (2) (2008) 255–260, https://doi.org/10.1002/pssa.200622541.

[7] J. Hüpkes, J. Owen, M. Wimmer, F. Ruske, D. Greiner, R. Klenk, U. Zastrow, J. Hotovy, Damp heat stable doped zinc oxide films, Thin Solid Films 555 (2014) 48–52, https://doi.org/10.1016/j.tsf.2013.08.011.

[8] D. Greiner, N. Papathanasiou, A. Pflug, F. Ruske, R. Klenk, Influence of damp heat on the optical and electrical properties of Al-doped zinc oxide, Thin Solid Films 517 (2009) 2291–2294, https://doi.org/10.1016/j.tsf.2008.10.107.

[9] D. Greiner, S. Gledhill, C. Köble, J. Krammer, R. Klenk, Damp heat stability of Al-doped zinc oxide films on smooth and rough substrates, Thin Solid Films 520 (2011) 1285–1290, https://doi.org/10.1016/j.tsf.2011.04.190.

[10] J. Steinhauser, S. Meyer, M. Schwab, S. Faÿ, C. Ballif, U. Kroll, D. Borrello, Humid environment stability of low pressure chemical vapor deposited boron doped zinc oxide used as transparent electrodes in thin film silicon solar cells, Thin Solid Films 520 (2011) 558–562, https://doi.org/10.1016/j.tsf.2011.06.095.

[11] T. Feurer, P. Reinhard, E. Avancini, B. Bissig, J. Löckinger, P. Fuchs, R. Carron, T. Weiss, J. Perrenoud, S. Stutterheim, S. Buecheler, A. Tiwari, Progress in thin film CIGS photovoltaics – Research and development, manufacturing, and applications, Prog. Photovoltaics Res. Appl 25 (2017) 645–667, https://doi.org/10.1002/pip.2811.

[12] M. Theelen, V. Hans, N. Barreau, H. Steijvers, Z. Vroon, M. Zeman, The impact of sodium and potassium on the degradation of CIGS solar cells, Prog. Photovoltaics Res. Appl. 23 (2015) 537–545, https://doi.org/10.1002/pip.2610.

[13] International Electrotechnical Commission. IEC 61215-1-4, Terrestrial photovoltaic (PV) modules – Design qualification and type approval – Part 1-4: Special requirements for testing of thin-film Cu(In,Ga)(S,Se)2 based photovoltaic (PV) modules.

[14] D. Greiner, Ursache der Leitfähigkeitsabnahme nach künstlicher Alterung in feuchter Warme bei hochdotierten Zinkoxid-Schichten für die Dünnschichtfotovoltaik, Ph.D. thesis, Freien Universität Berlin; 2010.

[15] J. Hüpkes, Influence of atmosphere and material properties on damp heat stability of ZnO:Al, P hysica Status Solidi A 213 (7) (2016) 1796–1800, https://doi.org/10.1002/pssa.201532966.

[16] J. Crank, The Mathematics of Diffusion, Oxford University Press, Oxford, UK, 1975.
[17] M. Theelen, C. Foster, S. Dasgupta, Z. Vroon, N. Barreau, M. Zeman, The influence of atmospheric species on the degradation of aluminum doped zinc oxide and Cu(In,Ga)Se_2 solar cells, in: Proc. SPIE, 9179, 2014, p. 91790K, https://doi.org/10.1117/12.2061330.
[18] M. Theelen, Degradation of CIGS solar cells, Ph.D. Thesis, Technical University of Delft; 2015.
[19] S. Schmidt, C. Wolf, H. Rodriguez-Alvarez, J.P. Bäcker, C. Kaufmann, S. Merdes, F. Ziem, M. Hartig, S. Cinque, I. Dorbandt, C. Köble, D. Abou-Ras, R. Mainz, R. Schlatmann, Adjusting the Ga grading during fast atmospheric processing of Cu(In,Ga)Se2 solar cell absorber layers using elemental selenium vapor, Prog. Photovolt: Res. Appl. 25 (2017) 341–357, https://doi.org/10.1002/pip.2865.
[20] M. Theelen, K. Beyeler, H. Steijvers, N. Barreau, Stability of CIGS Solar Cells under Illumination with Damp Heat and Dry Heat: A Comparison, Solar Energy Materials and Solar Cells 166 (2017) 262–268, https://doi.org/10.1016/j.solmat.2016.12.039.
[21] M. Theelen, N. Barreau, V. Hans, H. Steijvers, Z. Vroon, M. Zeman, Degradation of CIGS solar cells due to the migration of alkali-elements, Proc. 42nd IEEE PVSC (2015) 1–6, https://doi.org/10.1109/PVSC.2015.7355776.
[22] V. Fjällström, P. Salomé, A. Hultqvist, M. Edoff, T. Jarmar, B. Aitken, K. Zhang, K. Fuller, C. Kosik Williams, Potential-induced degradation of $CuIn_{1-x}Ga_xSe_2$ thin film solar cells, IEEE J. Photovolt. 3 (2013) 1090–1094, https://doi.org/10.1109/JPHOTOV.2013.2253833.
[23] O. Salomon, W. Hempel, O. Kiowski, E. Lotter, W. Witte, A. Ferati, A. Schneikart, G. Kaune, R. Schäffler, M. Becker, B. Schröppel, R. Vidal Lorbada, D. Mücke, T. Walter, Influence of Molybdenum Back Contact on the PID Effect for Cu(In,Ga)Se_2 Solar Cells, Coatings 9 (2019) 794, https://doi.org/10.3390/coatings9120794.